

Prediction of critical submergence for an intake pipe

Prédiction de l'immersion critique pour l'aspiration d'un tuyau

NEVZAT YILDIRIM, *Professor; Gazi University, Faculty of Engineering and Architecture, Civil Engineering Department, Maltepe, Ankara, Turkey*

FIKRET KOCABAŞ, *Assistant Professor; Erciyes University, Yozgat Faculty of Engineering and Architecture, Civil Engineering Department, Yozgat, Turkey*

ABSTRACT

In this study, the effects of the blockage of the intake pipe and impervious flow boundaries on critical submergence of an intake are presented. The potential solution based on the Rankine stagnation point is found to be an approximate method for the prediction of the critical submergence for an intake pipe. It is found that a critical spherical sink surface with a radius equal to the radial distance of the stagnation point (which is $1/\sqrt{2}$ times the critical submergence of the intake) can also be used to predict the critical submergence. The agreement between theoretical results and available experimental data indicates that this critical spherical sink surface gives good results especially for the intake when the distance of the impervious vertical dead-end wall to the center point of the intake is smaller than or equal to the diameter of the intake.

RÉSUMÉ

Dans cette étude, on présente l'influence de parois imperméables sur la profondeur critique d'immersion d'une prise. La solution en écoulement potentiel basée sur le point de stagnation de Rankine n'est qu'une méthode approximative de la prévision de l'immersion critique d'un tuyau de prise. On montre qu'une surface sphérique de puits, de rayon égal à la distance radiale du point d'arrêt (qui est $1/\sqrt{2}$ fois la profondeur d'immersion critique de la prise) peut être utilisé pour calculer l'immersion critique : la concordance des résultats théoriques et des données expérimentales disponibles montre que cette surface sphérique donne de bons résultats notamment dans le cas d'une prise proche de la paroi verticale d'un cul de sac de canal, lorsque la distance du centre de la prise à la paroi est inférieure ou égale au diamètre de la prise.

Introduction

Air-entrainment by means of a free air-core vortex occurring at intakes is one of the unsolved problems in hydraulic engineering. When the submergence of the intake is not sufficient, air enters the intake and can cause operational problems in the intake and affiliated systems (such as pumps; turbines etc..). The value of the submergence of the intake at which incipient air-entrainment is possible (the submergence for which the tip of the air-core is at the intake) is called the 'critical submergence' [Fig.1(b)]. There are several studies about the critical submergence of intakes (Anwar 1968, Jain et al. 1978, Odgaard 1986, Hite and Mih 1994 and Gulliver and Rindels 1987). In these studies, equation of motion of a real fluid differential-element in the vortex-core region is considered. Thus, the blockage effects of the intake pipe and impervious flow boundaries on the critical submergence are neglected. Recently, Yıldırım and Kocabaş (1995,1998,2000) have tried to predict the critical submergence by potential solution and by applying the continuity equation in a region far away from the vortex-core.

This study parallels that of Yıldırım et al. (2000). The main difference is that, in this study; the equation of the dividing stream surface and the Rankine stagnation point are approximated and a different critical spherical sink surface (CSSS) is defined to predict the critical submergence of the intake. The agreement between theoretical results and available experimental data indicates that this newly defined critical spherical sink surface gives good results especially for the intake when the distance of the impervi-

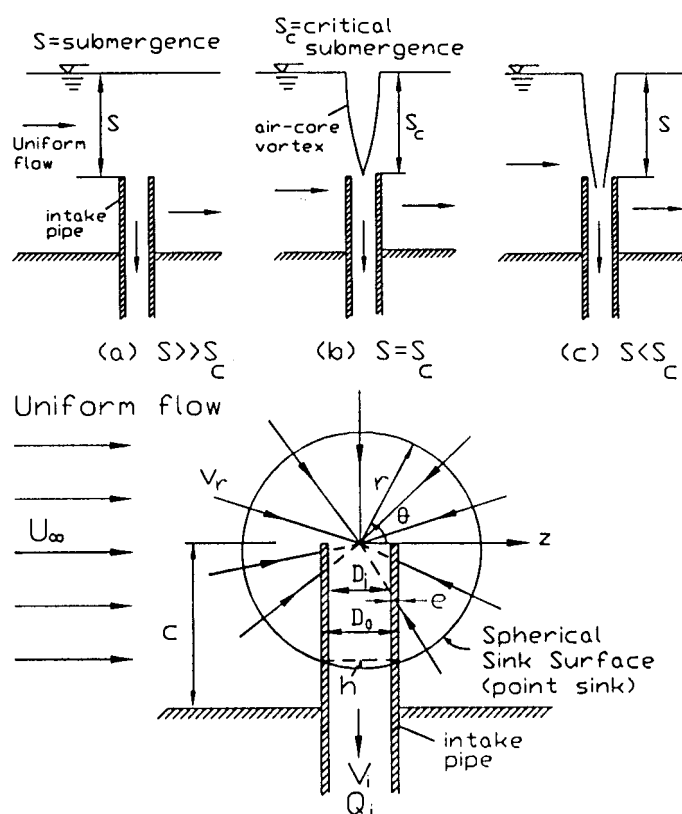


Fig. 1. Flow at the Intake (S = Submergence; S_c = Critical Submergence): (a) No Air-Core Vortex; (b) Air-Core Vortex just Reaches the Intake (Critical Condition); (c) Air-Entraining Vortex; (d) Combined Flow and Blockage of the Intake Pipe [Yıldırım et al. (2000)].

Revision received April 19, 2001. Open for discussion till December 31, 2002.

ous boundaries cutting the free surface to the center point of the intake is smaller than or equal to the diameter of the intake.

Theoretical consideration

In general, the critical submergence S_c for an intake can be predicted from the continuity equation [Yıldırım et.al. (2000)]

$$Q_i = A_c V_s = (\pi D_i^2/4) V_i \quad (1)$$

In which Q_i = intake discharge; A_c = the net total working surface area of the critical spherical sink surface (CSSS) under consideration after subtracting the blockage of all impervious boundaries and intake pipe; V_s = critical velocity at CSSS after subtracting the blockage; D_i = internal diameter of the intake pipe and V_i = average intake velocity. In general V_s has a constant value for a given flow and geometry and can be determined by conducting few experiments. In this study, the CSSS used by Yıldırım and Kocabaş (1995, 1998, 2000) is denoted as CSSS I which has a radius equal to the critical submergence, S_c , of the intake.

Since the blockage effects of the impervious boundaries on a small spherical sink surface are going to be smaller; it is better to utilize a spherical sink surface whose radius is less than S_c . But, the radius of the spherical sink surface and the velocity at it must be known in terms of S_c and approaching flow velocity. The stagnation point of the dividing stream surface has the smallest radial distance among all points on the dividing stream surface (if the distortion due to unsymmetrical flow is negligible). The radial distance of the stagnation point can be written in terms of S_c . Therefore, the stagnation point-based 'critical spherical sink surface' is a good choice for the prediction of the critical submergence especially in cases where the distances of the impervious boundaries to the center point of the intake are much smaller than the critical submergence. The prediction of the critical submergence based on the stagnation point is explained here after.

Consider an intake in a uniform flow. The intake flow is approximated as a point sink (spherical sink) as shown in Fig.1(d). For a combined potential flow of a point sink and a uniform flow, the total stream function ψ can be written as [Yuan (1967), eq.(7-136) is rewritten by considering the point sink in a uniform flow]

$$\psi = \frac{Q_i}{A_n} r^2 \cos\theta + \frac{1}{2} U_\infty r^2 \sin^2 \theta \quad (2)$$

In which A_n = the net working surface area of the spherical sink surface under consideration; θ = angle between horizontal axis z and radial direction vector (Fig.1); U_∞ = velocity of uniform canal flow at upstream of the intake and r = radial distance (radius of the spherical sink surface). By definition of radial velocity V_r [Yuan (1967), eq.(7-72)] and eq.(2) one can write

$$V_r = -\frac{1}{r^2 \sin\theta} \frac{\partial \psi}{\partial \theta} = \frac{Q_i}{A_n} - U_\infty \cos\theta \quad (3)$$

The main purpose is to find the equation of the dividing stream surface. If the blockages of the impervious flow boundaries and

the intake pipe were not present, the equation of the dividing stream surface would be the Rankine half-body of revolution [Yuan (1967)]. Because of the blockages of the impervious flow boundaries and the intake pipe, the spherical sink is not a complete spherical sink. Therefore, the dividing stream surface may be a little distorted in reality and may not be exactly the same as the Rankine half-body of revolution. Hence, the stagnation point of the dividing stream surface may not be exactly at $\theta = 0^\circ$. But one can expect that deviation of θ corresponding to the stagnation point should not be far off from 0° . Thus, for the stagnation point, one can approximately take $\cos \theta \approx 1$. Let r_s = radial distance of the stagnation point to the center of the intake and A_{ns} = value of A_n for $r = r_s$. At the stagnation point ($V_r = 0$, $r = r_s$, $\cos \theta \approx 1$) eq.(3) yields

$$Q_i = A_{ns} U_\infty \quad (4)$$

ψ takes the value of ψ_0 at the stagnation point [eq.(2)].

$$\psi_0 = \frac{Q_i r_s^2}{A_{ns}} \quad (5)$$

Hence, the equation of the dividing stream surface is therefore, [equating eqs.(2) and (5)],

$$\frac{Q_i}{A_n} r^2 \cos\theta + \frac{1}{2} U_\infty r^2 \sin^2 \theta = \frac{Q_i r_s^2}{A_{ns}} \quad (6)$$

Just above the intake $\theta = 90^\circ$ and $r = S_c$ (critical submergence for the intake) eq.(6) yields

$$Q_i = \left(\frac{A_{ns}}{r_s^2} S_c^2 \right) \frac{U_\infty}{2} \quad (7)$$

From eqs.(4) and (7) one obtains

$$S_c = \sqrt{2} r_s ; \quad \text{or} \quad \frac{S_c}{D_i} = \sqrt{2} \frac{r_s}{D_i} \quad (8)$$

It is clear that A_{ns} is the net total surface area of the critical spherical sink which is denoted as CSSS II in this study. Eqs. (4) or (7) and (8) show that the CSSS II has the radius of $r_s = S_c/\sqrt{2}$. At CSSS II, the velocity is equal to U_∞ . Eqs.(1), (4) or (7) and (8) indicate that $A_c = A_{ns}$ and $V_s = U_\infty$ or if $A_c = 2A_{ns}$ is taken $V_s = U_\infty/2$ which corresponds to the studies of Yıldırım and Kocabaş (1995, 1998, 2000).

Blockage of the intake pipe

The blockage of the intake pipe is equal to the surface area of the spherical sector (cap) of the CSSS II remaining inside the outer boundaries of the intake pipe where no flow is supplied to the intake. As shown in Fig.1, one can consider a spherical sink surface having radius of r for which the blockage of the intake pipe is present only for $c > (r-h)$. In which, c = clearance of the intake,

i.e., the vertical distance of the intake to the impervious canal bottom, and h = altitude of the spherical sector (cap) of the spherical sink surface remaining within the outer boundaries of the intake pipe. Considering Fig.1, from geometry one can write

$$(r - h)^2 + (D_0/2)^2 = r^2 \quad \text{or}; \quad h = r \left[1 - \sqrt{1 - 0.25(D_0/r)^2} \right] \quad (9)$$

In which, D_0 = outer diameter of the intake pipe. Let A_{pb} = blockage of the intake pipe for the spherical sink surface under consideration. From geometry (Fig.1) and eq.(9),

$$A_{pb} = 2\pi r h = 2\pi r^2 \left[1 - \sqrt{1 - 0.25(D_0/r)^2} \right] \quad (10)$$

$$A_n = 4\pi r^2 - A_{pb} = 2\pi r^2 \left[1 + \sqrt{1 - 0.25(D_0/r)^2} \right] \quad (11)$$

When $r = r_s$; $A_n = A_{ns}$. Eqs.(8) and (11) yield,

$$\begin{aligned} A_{ns} &= 2\pi r_s^2 \left[1 + \sqrt{1 - 0.25(D_0/r_s)^2} \right] \\ &= \pi S_c^2 \left[1 + \sqrt{1 - 0.5(D_0/D_i)^2 (D_i/S_c)^2} \right] \end{aligned} \quad (12)$$

$$A_{pb} = \pi S_c^2 \left[1 - \sqrt{1 - 0.5(D_0/D_i)^2 (D_i/S_c)^2} \right] \quad (13)$$

From eqs. (1), (7), (8) and (12) one obtains,

$$\frac{S_c}{D_i} = \frac{(V_i/U_\infty)^{1/2}}{2\sqrt{2} \sqrt{1 - \left(\frac{D_0}{D_i}\right)^2 \frac{U_\infty}{V_i}}} \quad (14)$$

From eqs.(7), (8) and (14) it yields

$$Q_i = 4\pi S_c^2 \left[1 - \left(\frac{D_0}{D_i}\right)^2 \frac{U_\infty}{V_i} \right] \frac{U_\infty}{2} \quad (15)$$

In eqs.(14) and (15), the term $(D_0/D_i)^2 (V_i/U_\infty)$ is due to the blockage of the intake pipe. If one takes the derivative of eq.(14) with respect to V_i/U_∞ and equate it to zero, it yields $V_i/U_\infty \geq 2(D_0/D_i)^2$. Replacing this result in eq.(14) gives the minimum value of

$$\frac{S_c}{D_i} = \frac{\sqrt{2}}{2} \left(\frac{D_0}{D_i}\right).$$

Hence, for the validity of the the potential solution (lower limit for the potential solution) the following condition should be satisfied.

$$\begin{aligned} \frac{V_i}{U_\infty} &> 2 \left(\frac{D_0}{D_i}\right)^2; \quad \frac{S_c}{D_i} = \frac{\sqrt{2}}{2} \left(\frac{D_0}{D_i}\right) \\ \frac{c}{D_i} &> \frac{S_c}{D_i} \frac{1}{\sqrt{2}} \sqrt{1 - 0.5 \left(\frac{D_0}{D_i}\right)^2 \left(\frac{D_i}{S_c}\right)^2} \end{aligned} \quad (16)$$

The potential solution assumes that the point of entry of the air-core vortex is the same as the center of the intake. But, in reality experiments have shown that for non-vertical intakes, the air-core vortex does not enter the intake from the center point of the intake [Yıldırım et al. (2000)]. For a horizontal intake the air-core vortex enters the intake from the point close to the summit point of the inner boundary of the intake. Therefore, lower limit of S_c/D_i is equal to minimum value of S_c/D_i found by potential solution plus the vertical distance between the point of entry of the air-core vortex and the center point of the intake. For a horizontal intake, the lower limit is $S_c/D_i \geq (\sqrt{2}/2)(D_0/D_i) + (D_i/2)/D_i = (\sqrt{2}/2)(D_0/D_i) + 0.5$. In the case of an intake in a still-water reservoir, since the flow field only consists of the point sink, one should replace U_∞ by V_s in eqs. (7), (14) and (15).

In order to see the effect of the blockage of the intake pipe on the critical submergence, the following should be done. When the blockage of the intake pipe is neglected eq.(14) gives

$$\left(\frac{S_c}{D_i}\right)_{wbp} = \frac{1}{2\sqrt{2}} \left(\frac{V_i}{U_\infty}\right)^{1/2} \quad (17)$$

In which the subscript 'wbp' stands for 'without blockage of the intake pipe'. The amount of error in S_c/D_i due to the blockage of the intake pipe can be computed from eqs. (14) and (17). It may be better to relate S_c/D_i to wall thickness of the intake pipe. Let e = wall thickness of the intake pipe (Fig.1).

$$D_0 = D_i + 2e \quad \text{or} \quad \frac{D_0}{D_i} = 1 + 2\frac{e}{D_i} \quad (18)$$

In which e/D_i = relative wall thickness of the intake pipe. The amount of error is [from eqs.(14), (17) and (18)]

$$\frac{\left(\frac{S_c}{D_i}\right) - \left(\frac{S_c}{D_i}\right)_{wbp}}{\left(\frac{S_c}{D_i}\right)_{wbp}} = \frac{1}{\sqrt{1 - \left(1 + 2\frac{e}{D_i}\right)^2 \frac{U_\infty}{V_i}}} - 1 \quad (19)$$

For different values of e/D_i , eq.(19) is graphically presented in Fig.2 which shows that as the wall thickness increases significantly, the intake behaves as if it was located at the bottom of the canal.

Blockage of impervious canal boundaries

Consider an intake (Fig.3) in a dead-end horizontal canal whose boundaries (side walls and dead-end) are vertical. There may or

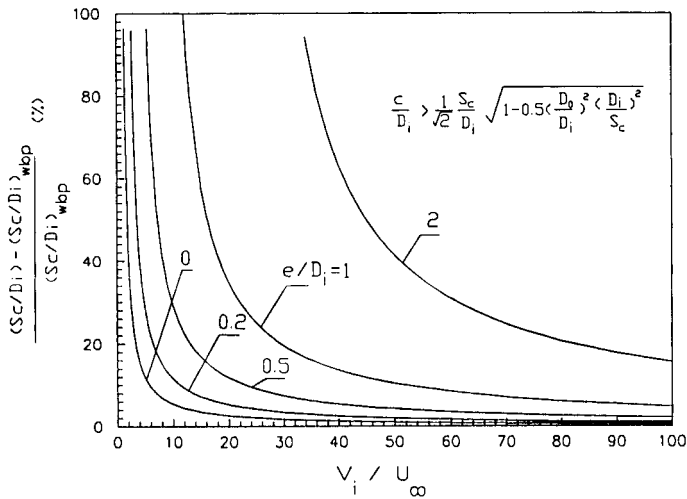


Fig. 2. Error in critical submergence due to blockage of the intake pipe (for CSSS II).

may not be flow over the dead-end wall. The center point of the intake is marked as M in Fig.3. From geometry, various surface section areas of the complete CSSS II in Fig.3 may be written as,

$$\begin{aligned}
 NFG &= 2\pi r_s(r_s - c); & S_1Z_1B_1 &= 2\pi r_s \overline{K_1Z_1} \\
 N_1IS_1B_1 &= 2\pi r_s(r_s - b_1); & S_2Z_2B_2 &= 2\pi r_s \overline{K_2Z_2} \\
 FGL &= 2\pi r_s(r_s - l); & S_3Z_3B_3 &= 2\pi r_s \overline{K_3Z_3}; & FHG &= 2\pi r_s \overline{JH}; \\
 S_4Z_4B_4 &= 2\pi r_s \overline{K_4Z_4}; & N_2RS_2B_2 &= 2\pi r_s(r_s - b_2)
 \end{aligned} \quad (20)$$

Where l = horizontal distance of the center point of the intake to the vertical dead-end; b_1 = horizontal distance of the center point of the intake to the vertical right side wall of the canal and b_2 = horizontal distance of the center point of the intake to the vertical left side wall of the canal. Let A_{bb} = the total blockage surface area of the impervious canal boundaries. Then, from Fig. 3

$$\begin{aligned}
 A_{bb} &= NFG + (FGL - FHG) + [N_1IS_1B_1 \\
 &\quad - (S_1Z_1B_1 + S_3Z_3B_3)] \\
 &\quad + [N_2RS_2B_2 - (S_2Z_2B_2 + S_4Z_4B_4)]
 \end{aligned} \quad (21)$$

By following exactly the same procedure as that of Yildirim et al. (2000), except the radius of the CSSS is taken as $r_s = S_c/\sqrt{2}$ instead of S_c , from eqs. (20) and (21) one can find,

$$\begin{aligned}
 A_{bb} &= 4\pi S_c^2 - \sqrt{2} \pi S_c (c + b_1 + b_2 + l) \\
 &\quad - \sqrt{2} \pi S_c (\overline{JH} + \overline{K_1Z_1} + \overline{K_2Z_2} + \overline{K_3Z_3} + \overline{K_4Z_4})
 \end{aligned} \quad (22)$$

As it is seen in Fig.3. \overline{JH} = altitude of the spherical sector (FHG) of the CSSS II due to the common blockages of the canal bottom and the dead-end wall, $\overline{K_1Z_1}$ and $\overline{K_2Z_2}$ are the altitudes of the spherical sectors ($S_1Z_1B_1$ and $S_2Z_2B_2$) of the CSSS II due to the common blockages of the dead-end wall and the right side wall and left side wall of the canal respectively, $\overline{K_3Z_3}$ and $\overline{K_4Z_4}$ are the altitudes of the spherical sectors ($S_3Z_3B_3$ and $S_4Z_4B_4$) of the CSSS II due to the common blockages of the canal bottom and the right side wall and left side wall of the canal accordingly. \overline{JH} , $\overline{K_1Z_1}$, $\overline{K_2Z_2}$, $\overline{K_3Z_3}$, $\overline{K_4Z_4}$ and the expressions given below are provided in Appendix I.

$$\begin{aligned}
 (S_c/D_i)^2 \leq 2 \left[(c/D_i)^2 + (l/D_i)^2 \right]; & \quad \overline{JH} = 0 \\
 (S_c/D_i)^2 \leq 2 \left[(b_1/D_i)^2 + (l/D_i)^2 \right]; & \quad \overline{K_1Z_1} = 0 \\
 (S_c/D_i)^2 \leq 2 \left[(b_2/D_i)^2 + (l/D_i)^2 \right]; & \quad \overline{K_2Z_2} = 0 \\
 (S_c/D_i)^2 \leq 2 \left[(c/D_i)^2 + (b_1/D_i)^2 \right]; & \quad \overline{K_3Z_3} = 0 \\
 (S_c/D_i)^2 \leq 2 \left[(c/D_i)^2 + (b_2/D_i)^2 \right]; & \quad \overline{K_4Z_4} = 0
 \end{aligned} \quad (23)$$

If the distance of an impervious flow boundary to the intake center is larger than or equal to r_s (or $S_c/\sqrt{2}$) the blockage of this solid boundary will be neglected (its blockage is not present). Considering Fig.3, it is clear that whichever of c , b_1 , b_2 and l is greater than or equal to r_s (or $S_c/\sqrt{2}$) it will be set equal to $r_s = S_c/\sqrt{2}$ in eqs.(22) and (23). Except the one belonging to the impervious flow boundary through which the intake pipe passes [due to similar reason of $r = r_s$, $c > (r_s - h)$], if it is greater than or equal to $(S_c/\sqrt{2}) \sqrt{1 - 0.5(D_0/D_i)^2 (D_i/S_c)^2}$ it will be set equal to $(S_c/\sqrt{2}) \sqrt{1 - 0.5(D_0/D_i)^2 (D_i/S_c)^2}$. If the distance of an impervious flow boundary through which the intake pipe passes is larger than or equal to $(S_c/\sqrt{2}) \sqrt{1 - 0.5(D_0/D_i)^2 (D_i/S_c)^2}$ the blockage of the impervious boundary is not present but the blockage of the intake

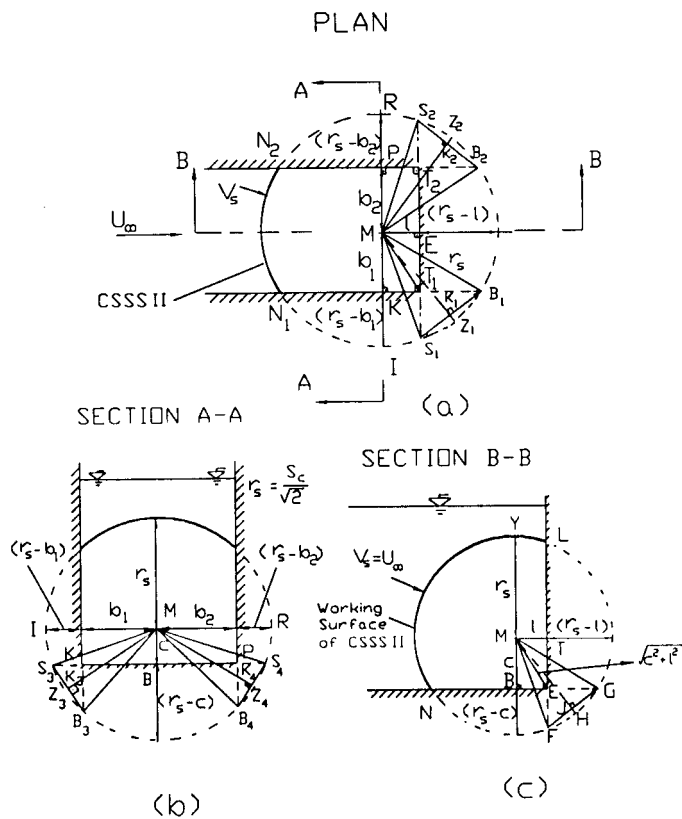


Fig. 3. Blockage of impervious flow boundaries (for CSSS II).

pipe is present ($A_{pb} \neq 0$). From eqs.(22) and (23) one can compute A_{bb} .

$$A_c = 4\pi r_s^2 - [A_{bb} + A_{pb}] \quad (24)$$

Depending on flow and geometry, due to the reasons explained above, A_{bb} and A_{pb} may or may not be present together [more details are given in the study of see Yıldırım et al. (2000)]. Due to eqs.(1) and (4) or (7) and (8), for practice one can approximate V_s as (if $A_c = A_{ns}$ is considered);

$$V_s = U_\infty \quad (25)$$

From eqs. (1), (22), (24) and (25) one can compute S_c/D_i by a trial-error method.

For general flow conditions and positions of an intake one should follow the same procedure as explained before and compute the total blockage of flow boundaries and intake pipe ($A_{bb}+A_{pb}$) and A_c . Then, S_c has to be calculated from A_c in eq.(1).

Comparison of theoretical and experimental results

The results of CSSS I and CSSS II and available experimental data of Iversen (1953), Yıldırım et al. (2000), Yıldırım and Jain (1979) and Gulliver and Rindels (1987) are compared in Tables

1, 2, 3 and 4 and in Fig. 4. Note that due to eq. (23), in all these experimental works $\overline{K_1 Z_1} = 0$; $\overline{K_2 Z_2} = 0$, $\overline{K_3 Z_3} = 0$, $\overline{K_4 Z_4} = 0$. Details are given in Tables 1, 2, 3 and 4.

The potential solution assumes that the point of entry of the air-core vortex is the same as the center of the intake. But, in reality experiments have shown that for non-vertical intakes, the air-core vortex does not enter the intake from the center point of the intake. For a horizontal intake the air-core vortex enters the intake from the point close to the summit point of the inner boundary of the intake. It is understood that in order to predict the critical submergence for a real fluid case, the vertical difference between the point of entry of the air-core vortex and the center point of the intake must be subtracted from the value of the critical submergence computed by means of potential solution. This is why theoretical values of the critical submergence in Table.1 are obtained by subtracting $D_i/2$ from values of S_c/D_i computed by means potential solution. As it is seen in these tables, as the intake discharge, Q_i , or intake velocity, V_i , gets smaller the difference between the theoretical and experimental results increases. This is due to unsteadiness of vortex motion in very low circulation.

Denny (1957) have conducted experiments for different vertical intake pipes sited at the center of square sumps ranging in width from 6" (15.24 cm) to 8 ft (244 cm) and examined the effect of the imposed rotation on the critical submergence. The approaching flow in his experiments was not a uniform flow. Due to this rea-

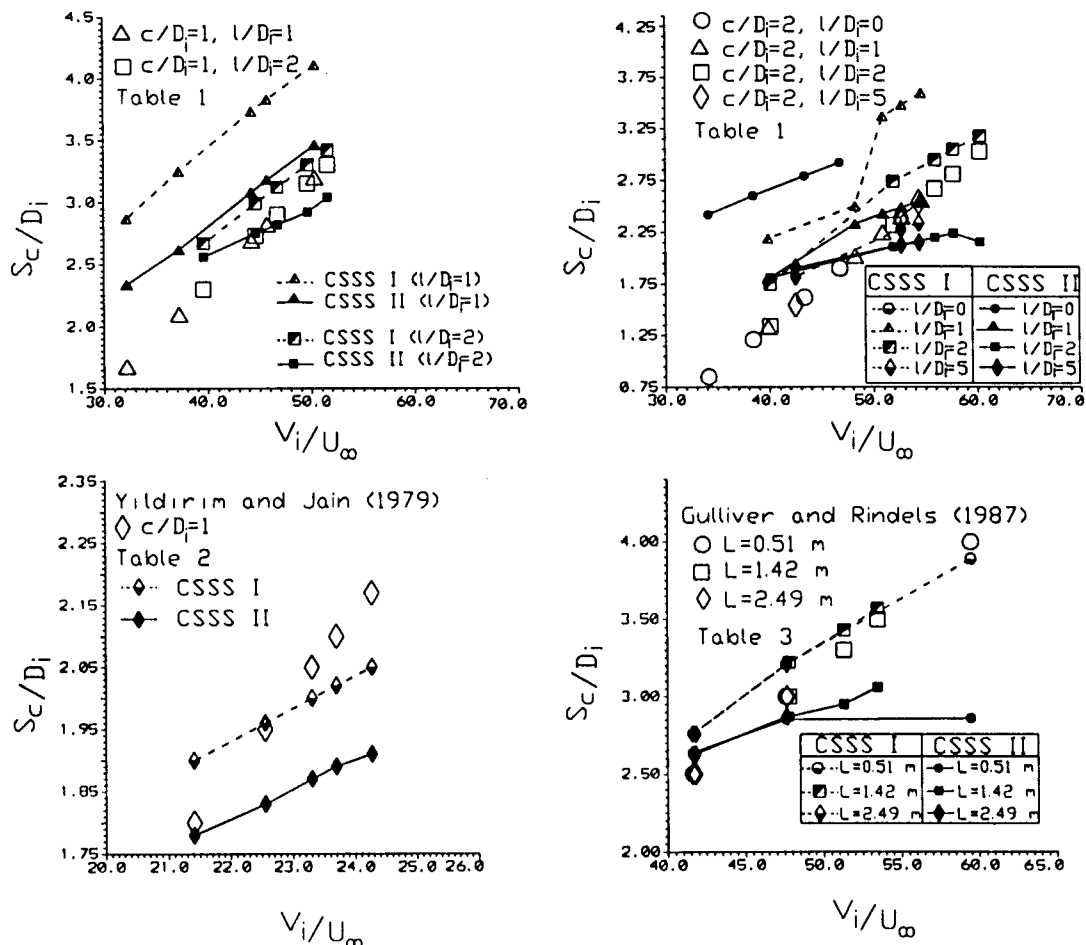


Fig. 4. Graphical comparison of CSSS I, CSSS II and Experimental Data.

Tabel 1 Experimental data on critical submergence for a horizontal intake passing through the dead-end.

Experiment						Yıldırım et al. (2000)	Eqs.(1), (22), (24) and (25) in this paper		
$\frac{c}{D_i}$	$\frac{l}{D_i}$	Q_i (l/s)	Flow Depth (cm)	$\frac{V_i}{U_\infty}$	$\frac{S_c}{D_i}$	CSSS I S_c/D_i^{**}	CSSS II S_c/D_i^{**}	Comment	
(1)	(2)	(3)	(4)	(5)	(6)	(7)	(8)	(9)	
1	1	10.04	22.35	50.30	3.20	4.11	3.46	$\overline{JH} \neq 0; A_{pb}=0; c/D_i=1; l/D_i=1$	
		7.07	20.30	45.70	2.82	3.83	3.18	$\overline{JH} \neq 0; A_{pb}=0; c/D_i=1; l/D_i=1$	
		4.71	19.65	44.20	2.69	3.73	3.08	$\overline{JH} \neq 0; A_{pb}=0; c/D_i=1; l/D_i=1$	
		2.64	16.50	37.18	2.10	3.25	2.62	$\overline{JH} \neq 0; A_{pb}=0; c/D_i=1; l/D_i=1$	
		1.39	14.25	32.17	1.68	2.87	2.34	$\overline{JH} \neq 0; A_{pb}=0; c/D_i=1; l/D_i=1$	
	2	-	-	-	-	-	-	-	-
		10.04	22.90	51.55	3.30	3.42	3.04	$\overline{JH} \neq 0; A_{pb}=0; c/D_i=1; l/D_i=2$	
		5.88	22.05	49.60	3.15	3.30	2.92	$\overline{JH} \neq 0; A_{pb}=0; c/D_i=1; l/D_i=2$	
		3.89	20.75	46.71	2.90	3.12	2.82	$\overline{JH} = 0; A_{pb} \neq 0; c/D_i=1; l/D_i=(S_c/D_i) \Delta^*$	
		2.38	19.85	44.60	2.73	2.99	2.75	$\overline{JH} = 0; A_{pb} \neq 0; c/D_i=1; l/D_i=(S_c/D_i) \Delta^*$	
	0	-	-	-	-	-	-	-	-
		10.13	20.75	46.70	1.90	2.92	2.92	$\overline{JH} = 0; A_{pb}=0; c/D_i=(S_c/D_i)/\sqrt{2}; l/D_i=0$	
		7.22	19.25	43.31	1.62	2.79	2.79	$\overline{JH} = 0; A_{pb}=0; c/D_i=(S_c/D_i)/\sqrt{2}; l/D_i=0$	
		4.16	17.05	38.39	1.21	2.60	2.60	$\overline{JH} = 0; A_{pb}=0; c/D_i=(S_c/D_i) \sqrt{2}; l/D_i=0$	
		2.21	15.15	34.10	0.85	2.42	2.42	$\overline{JH} = 0; A_{pb}=0; c/D_i=(S_c/D_i)/\sqrt{2}; l/D_i=0$	
2	1	-	-	-	-	-	-	-	
		10.04	24.25	54.55	2.56	3.60	2.55	$\overline{JH} = 0; A_{pb}=0; c/D_i=(S_c/D_i)/\sqrt{2}; l/D_i=1$	
		6.42	23.40	52.67	2.40	3.48	2.49	$\overline{JH} = 0; A_{pb}=0; c/D_i=(S_c/D_i)/\sqrt{2}; l/D_i=1$	
		3.75	22.60	50.84	2.25	3.37	2.43	$\overline{JH} = 0; A_{pb}=0; c/D_i=(S_c/D_i)/\sqrt{2}; l/D_i=1$	
		2.55	21.40	48.17	2.02	2.50	2.33	$\overline{JH} = 0; A_{pb}=0; c/D_i=(S_c/D_i)/\sqrt{2}; l/D_i=1$	
	2	-	-	-	-	-	-	-	-
		10.13	26.75	60.21	3.03	3.18	2.16	$\overline{JH} = 0; A_{pb}=0; c/D_i=2; l/D_i=2$	
		6.99	25.60	57.66	2.81	3.05	2.24	$\overline{JH} = 0; A_{pb} \neq 0; c/D_i=(S_c/D_i)/\sqrt{2}; l/D_i=(S_c/D_i) \Delta^*$	
		4.83	24.85	55.89	2.67	2.95	2.20	$\overline{JH} = 0; A_{pb} \neq 0; c/D_i=(S_c/D_i)/\sqrt{2}; l/D_i=(S_c/D_i) \Delta^*$	
		2.71	23.00	51.87	2.32	2.74	2.11	$\overline{JH} = 0; A_{pb} \neq 0; c/D_i=(S_c/D_i)/\sqrt{2}; l/D_i=(S_c/D_i) \Delta^*$	
	5	-	-	-	-	-	-	-	-
		10.04	24.15	54.35	2.54	2.34	2.15	$\overline{JH} = 0; A_{pb} \neq 0; c/D_i=(S_c/D_i)/\sqrt{2}; l/D_i=(S_c/D_i) \Delta^*$	
		2.78	23.35	52.61	2.39	2.28	2.13	$\overline{JH} = 0; A_{pb} \neq 0; c/D_i=(S_c/D_i)/\sqrt{2}; l/D_i=(S_c/D_i) \Delta^*$	
		0.76	18.87	42.48	1.55	1.82	1.90	$\overline{JH} = 0; A_{pb} \neq 0; c/D_i=(S_c/D_i)/\sqrt{2}; l/D_i=(S_c/D_i) \Delta^*$	
		-	-	-	-	-	-	-	-

Note: From Yıldırım et. al.(2000), $D_i = 5.32$ cm., $D_0 = 5.92$ cm., $e = 3$ mm., $b_1 = b_2 = 25$ cm.

** S_c/D_i from potential solution - $(D_i/2)/D_i$; $\Delta^* = (1/\sqrt{2})\sqrt{1 - 0.5(D_0/D_i)^2(D_i/S_c)^2}$

son, V_s can not be known in terms of U_∞ so as to compare his experimental results with this study [V_s is not known in advance for his study, if wanted one can determine V_s for his study by means of eq. (1) for both CSSS I and CSSS II. Besides, he has given envelope curves and omitted the test points (Figs.4-14)]. It is clear that this study can not be compared with the results of Denny (1957). On the other hand, in the study of Iversen (1953) it is stated that ‘the approaching flow to the intake was parallel to the side walls’ (uniform flow). Therefore, the experimental results of Iversen (1953) are comfortably compared with this study. He has used a vertical intake pipe flowing vertically upward in a dead-end canal with uniform approaching flow. In his experiments the inner diameter of the intake pipe and the inner diameter of the bell are $D_i = 10.80$ cm and $D_{bi} = 16.20$ cm respectively. The wall thickness of the intake pipe is not given. It is a common steel pipe whose wall thickness is approximated to be about $e = 5$ mm. Therefore, the outer diameter of the intake pipe is $D_0 = D_i + 2e = 11.80$ cm. First few experimental results given in Table 2 of Iversen (1953) are compared with this study as shown in Table

4. Since Iversen has used the internal diameter of the bell, D_{bi} , for non-dimensional quantities in his Table 2, same D_{bi} is used for the non-dimensional quantities in Table 4 of this study. In reality; as far as the continuity is concerned, it doesn’t matter whether one uses the internal diameter of the bell or the internal diameter of the intake pipe. But; in the cases where the blockage of the intake pipe is present, the outer diameter of the intake pipe, D_0 , is considered in the blockage term of the intake pipe. In the study of Iversen (1953), the blockage of the intake pipe is always present [although it is negligibly small since e is small, see Fig.6 of Yıldırım et al.(2000)]. Note that in Table 4, the symbols used in Table 2 of Iversen are replaced with the corresponding symbols used in this study. Due to eq.(16) of Yıldırım et al. (2000) and similar eq.(23) in this study, for both CSSS I and CSSS II, in the experimental results of Iversen (1953, Table 2), $\overline{JH} = 0; K_1Z_1 = 0; K_2Z_2 = 0; K_3Z_3 = 0; K_4Z_4 = 0. A_{pb} \neq 0$. Hence, for CSSS I and for the experimental results of Iversen (1953), from eqs.(19) and (22) of Yıldırım et al.(2000) one obtains (replacing D_i by D_{bi})

Table 2 Experimental data on critical submergence for a vertical downward intake in a dead-end canal.

Experiment		Computed		Yıldırım et al. (2000)	Eqs.(1), (22), (24) and (25) in this paper
Q _i (l/s) (1)	Flow depth (cm) (2)	S _c /D _i (3)	V _i /U _∞ (4)	CSSS I S _c /D _i (5)	CSSS II S _c /D _i (6)
3.40	14.22	1.80	21.407	1.90	1.78
3.80	14.99	1.95	22.554	1.96	1.83
4.40	15.49	2.05	23.306	2.00	1.87
4.50	15.75	2.10	23.698	2.02	1.89
5.10	16.13	2.17	24.269	2.05	1.91

Note: From Yıldırım and Jain (1979), data on c/D_i = 1 curve, air vortex, pure water, D_i = 5.08 cm, D₀ = 5.68 cm, canal width = 30.48 cm, l = 30 cm, b₁ = b₂ = 15 cm. $\overline{JH} = \overline{K_1 Z_1} = \overline{K_2 Z_2} = \overline{K_3 Z_3} = \overline{K_4 Z_4} = 0$; b₁ and b₂ are set equal to S_c/√2; A_{pb} ≠ 0.

Table 3 Experimental data on critical submergence for a vertical upward intake in a dead end canal.

Experiment			Computed	Yıldırım et al. (2000)	Eqs.(1), (22), (24) and (25) in this paper	
Figure (1)	S _c /D _i (2)	F (3)	V _i /U _∞ (4)	CSSS I S _c /D _i (5)	CSSS II S _c /D _i (6)	Comment (7)
Fig.7	4.0	1.80	59.45	3.89	2.86	A _{pb} =0; \overline{JH} =0; l/D _i =2.67; c/D _i =1
α=0	3.0	1.20	47.59	3.21	2.85	A _{pb} ≠0; \overline{JH} =0; l/D _i =(1/√2)S _c /D _i ; c/D _i =1
L=0.51m	2.5	0.30	41.62	2.76	2.64	A _{pb} ≠0; \overline{JH} =0; l/D _i =(1/√2)S _c /D _i ; c/D _i =1
N _r '=0	-	-	-	-	-	-
Fig.8	3.5	1.40	53.56	3.57	3.06	A _{pb} ≠0; \overline{JH} =0; l/D _i =(1/√2)S _c /D _i ; c/D _i =1
α=0	3.5	0.90	53.45	3.57	3.06	A _{pb} ≠0; \overline{JH} =0; l/D _i =(1/√2)S _c /D _i ; c/D _i =1
L=1.42m	3.3	0.60	51.29	3.43	2.95	A _{pb} ≠0; \overline{JH} =0; l/D _i =(1/√2)S _c /D _i ; c/D _i =1
N _r '=0	3.0	0.30	47.78	3.22	2.87	A _{pb} ≠0; \overline{JH} =0; l/D _i =(1/√2)S _c /D _i ; c/D _i =1
Fig.9	3.0	2.30	47.63	3.21	2.87	A _{pb} ≠0; \overline{JH} =0; l/D _i =(1/√2)S _c /D _i ; c/D _i =1
α=0	2.5	0.80	41.61	2.76	2.63	A _{pb} ≠0; \overline{JH} =0; l/D _i =(1/√2)S _c /D _i ; c/D _i =1
L=2.49m	2.5	0.45	41.80	2.76	2.63	A _{pb} ≠0; \overline{JH} =0; l/D _i =(1/√2)S _c /D _i ; c/D _i =1
N _r '=0	-	-	-	-	-	-

Note : From Gulliver and Rindels (1987); Figs. 7-9, vane angle α = 0; far field circulation = 0, N_r' = 0 (representing uniform flow), D_i = 0.15 m, c/D_i = 1, canal width 1.4 m, bell-mouth intake, uppermost data just under the envelope curve, b₁ = b₂ = 70 cm, l = 40 cm.

Table 4. Experimental data on critical submergence for a vertical intake flowing upward in a dead-end canal.

Experiment										This study	
Run No.	$\frac{b_1}{D_{bi}}$	$\frac{b_2}{D_{bi}}$	$\frac{c}{D_{bi}}$	$\frac{l}{D_{bi}}$	Q_i (l/s)	Flow Depth (cm)	Canal width (b ₁ +b ₂) (cm)	$\frac{V_i}{U_\infty}$	$\frac{S_c}{D_{bi}}$	CSSS I S_c/D_{bi} [eq.(26)]	CSSS II S_c/D_{bi} [eq.(27)]
(1)	(2)	(3)	(4)	(5)	(6)	(7)	(8)	(9)	(10)	(11)	(12)
53	1	1	0.50	1	13.90	27.20	32.40	4.30	1.18	1.30	0.90
31	1	1	1	1	13.90	31.80	32.40	5.00	0.96	0.82	0.82
68	1	1	2	1	13.90	44.20	32.40	6.95	0.73	0.95	0.95
50	1.50	1.50	0.50	1.50	13.90	29.00	48.60	6.84	1.29	1.13	1.17
30	1.50	1.50	1	1.50	13.90	33.50	48.60	7.91	1.07	1.02	1.01
63	1.50	1.50	2	1.50	13.90	50.40	48.60	11.89	1.11	1.23	1.23
45	2.50	2.50	0.50	2.50	13.90	48.90	81.00	19.23	2.52	3.20	2.04
37	2.50	2.50	1	2.50	13.90	42.60	81.00	16.76	1.63	1.62	1.74

Note: From Iversen (1953), Table 2.

$$\frac{1}{4} \left(\frac{D_{bi}}{S_c} \right) \frac{V_i}{U_\infty} + 3 \frac{S_c}{D_{bi}} - \left(\frac{S_c}{D_{bi}} \sqrt{1 - 0.25 \left(\frac{D_0}{D_{bi}} \right)^2 \left(\frac{D_{bi}}{S_c} \right)^2} + \left(\frac{c}{D_{bi}} + \frac{b_1}{D_{bi}} + \frac{b_2}{D_{bi}} + \frac{l}{D_{bi}} \right) \right) = 0 \quad (26)$$

As shown by Yildirim et al.(2000), notice that for CSSS I, whichever of c, b₁, b₂ and l is larger than or equal to S_c, it will be set equal to S_c [except the one belonging to the impervious flow boundary through which the intake pipe passes. If it is greater than or equal to S_c√(1-0.25(D₀/D_i)²(D_i/S_c)²), it will be taken to be equal to S_c√(1-0.25(D₀/D_i)²(D_i/S_c)²). Note that for the comparison of data of Iversen (1953), D_i is replaced with D_{bi} due to the reason explained before.

For CSSS II and for the experimental results of Iversen (1953), from eqs.(1), (8), (13), (22), (23), (24) and (25) one obtains

[by taking 0.5 = 0.25 (√2)²].

$$\frac{1}{4} \left(\frac{D_{bi}}{S_c} \right) \frac{V_i}{U_\infty} + 3 \frac{S_c}{D_{bi}} - \left(\frac{S_c}{D_{bi}} \sqrt{1 - 0.25 (\sqrt{2})^2 \left(\frac{D_0}{D_{bi}} \right)^2 \left(\frac{D_{bi}}{S_c} \right)^2} + \sqrt{2} \left(\frac{c}{D_{bi}} + \frac{b_1}{D_{bi}} + \frac{b_2}{D_{bi}} + \frac{l}{D_{bi}} \right) \right) = 0 \quad (27)$$

As mentioned before, for CSSS II, whichever of c, b₁, b₂ and l is greater than or equal to r_s (or S_c/√2) it will be set equal to r_s = S_c/√2. Except the one belonging to the impervious flow boundary through which the intake pipe passes, if it is greater than or equal to (S_c/√2)√(1-0.5(D₀/D_i)²(D_i/S_c)²) it will be set equal to (S_c/√2)√(1-0.5(D₀/D_i)²(D_i/S_c)²). Eqs. (26) and (27) are solved for S_c/D_{bi} by a trial-and-error method and the results are presented in Table 4.

Comparison of results of CSSS I and CSSS II

As it was mentioned before, CSSS I and CSSS II have radiuses of S_c and S_c/√2 respectively. CSSS I and CSSS II have the same discharge and center as the intake. In order to see the difference between CSSS I and CSSS II, as an example; one can consider the eqs.(1) and (25) when only the blockage of the canal bottom present.

For CSSS I [Yildirim and Kocabaş (1995,1998,2000)];

$$Q_i = 2\pi S_c (S_c + c) U_\infty / 2$$

or;

$$\frac{S_c}{D_i} = \frac{-c/D_i + \sqrt{(c/D_i)^2 + V_i/U_\infty}}{2} \quad (28)$$

For CSSS II;

$$Q_i = 2\pi r_s (r_s + c) U_\infty = 2\pi S_c (S_c + \sqrt{2} c) U_\infty / 2$$

$$= [4\pi S_c^2 - 2\pi S_c (S_c - \sqrt{2} c)] U_\infty / 2 \quad (29)$$

$$\frac{S_c}{D_i} = \frac{-\sqrt{2}(c/D_i) + \sqrt{2(c/D_i)^2 + V_i/U_\infty}}{2}$$

For the cases of $c = 0$ and $c \geq S_c/\sqrt{2}$ (since c is set equal to $S_c/\sqrt{2}$) eq.(28) gives

$$\begin{aligned} Q_i &= (2\pi S_c^2)U_\infty/2; & (c = 0) \\ Q_i &= (4\pi S_c^2)U_\infty/2; & (c \geq S_c/\sqrt{2}) \end{aligned} \quad (30)$$

Eqs. (29) and (30) infer that one can also consider a CSSS that has a radius of S_c which is CSSS I. It is clear that both CSSS I and CSSS II are present and both can be used. If one compares eqs. (26) and (27), and eqs.(28) and (30) it is seen that the only difference is in the factors of blockage terms. The factors of blockage terms for CSSS I and CSSS II are 1 and $\sqrt{2}$ respectively. The factor of blockage depends on which spherical sink surface is considered as CSSS. The aforementioned results suggest that in general one can choose any spherical sink surface as CSSS provided that the velocity at the CSSS, factor of blockage for the CSSS and the radius of the CSSS in terms of S_c are known. One may wonder which one of CSSS I and CSSS II is to be preferred. This point may be explained as follows.

When distances of impervious solid boundaries to the intake get smaller than S_c , they cut the CSSS and cause considerable region of vorticity (smaller distance means larger region of vorticity) within and on the CSSS. The curvature of the streamlines close to boundaries increases so much (in these regions assumptions of radial point sink flow and uniform flow fail). The effects of Reynolds number, Weber number and Kolf number (circulation number) on the phenomenon become considerably large. It is understood that whichever of CSSS I and CSSS II is least affected by the impervious flow boundaries (blockage effect, vorticity effect and the curvature effects on the streamlines) that one is preferred. As it will be seen in Tables 1, 2, 3 and 4, both CSSS I and CSSS II give close and acceptable results. Therefore, in practice any one of CSSS I and CSSS II can be used. The results in Tables 1, 2, 3 and 4 show that CSSS I predicts S_c little better than CSSS II for the case of $l/D_i > 1$ on the other hand CSSS II predicts S_c better than CSSS I for the case of $0 < l/D_i \leq 1$. As mentioned, these results are due to the locations and effects of the impervious boundaries (i.e. for the case of $0 < l/D_i \leq 1$, blockage effects, vorticity effects and the curvature effects of the boundaries on the CSSS I are apparently more than that on the CSSS II. As for the case of $l/D_i > 1$ it is the opposite).

Conclusions

In this study, by means of a potential solution, it is found that a critical spherical sink surface (CSSS II) with a radius equal to the radial distance of the stagnation point (which is $1/\sqrt{2}$ times the critical submergence of the intake) can also be used to predict the critical submergence. The effects of the blockage of the intake pipe and impervious flow boundaries on critical submergence of an intake are presented. The agreement between theoretical results and available experimental data indicates that when the distance (l) of the vertical dead-end wall is smaller than or equal to the diameter (D_i) of the intake ($0 < l/D_i \leq 1$), the CSSS II predicts the critical submergence (S_c) better than CSSS I. For other cases ($1 < l/D_i < S_c/D_i$) CSSS I predicts the critical submergence (S_c)

better than CSSS II. When the distances of impervious boundaries to the center point of the intake are all zero and are all larger than or equal to the critical submergence; CSSS I and CSSS II give same results (critical submergence). CSSS I predicts S_c on safe side. Results of CSSS I and CSSS II are not far off. Therefore, both CSSS I and CSSS II can be used to predict the critical submergence for an intake pipe.

Notations

A_{bb}	total blockage of impervious flow boundaries (except the intake pipe)
A_c	total net working surface area of the CSSS
A_n	total net working surface area of spherical sink surface
A_{ns}	value of A_n for $r = r_s = S_c/\sqrt{2}$
A_{pb}	blockage of the intake pipe
b_1	horizontal distance of the center point of the intake to right side wall of the canal
b_2	horizontal distance of the center point of the intake to left side wall of the canal
c	clearance (vertical distance of the intake to bottom of canal)
D_{bi}	internal diameter of the bell
D_i	internal diameter of intake pipe
D_0	outer diameter of intake pipe
e	wall thickness of the intake pipe
F	Froude number = $V_i/(gD_i)^{0.5}$
g	gravity acceleration
h	altitude of the spherical sector (cap) of a spherical sink
l	horizontal distance of the center point of the intake to impervious dead-end
Q_i	intake discharge = $V_i \pi D_i^2/4$
r	radial distance
r_s	radial distance of the stagnation point
S_c	critical submergence (critical value of S)
U_∞	velocity of uniform canal flow at upstream of intake
V_i	average intake velocity
V_r	total radial velocity
V_s	critical radial velocity at CSSS
z	horizontal axis
θ	angle between r and z
ψ	total stream function
ψ_0	value of ψ at the stagnation point

References

- ANWAR, H.O. (1968). Prevention of vortices at intakes. *Water Power*, (October.), p.393-401.
- DENNY, D.F., and YOUNG, A.J. (1957). The prevention of vortices and swirl at intakes. *Proceedings of the 7th International Association for Hydraulic Research (IAHR)*, Vol.1, paper C1, Lisbon.
- GULLIVER, S.J., and RINDELS, A.J. (1987). Weak vortices at vertical intakes. *Journal of Hydraulic Engineering*, ASCE, Vol.113, No.9, p. 1101-1116.
- IVERSEN, H.W. (1953). Studies of submergence requirements of high-specific-speed pumps. *Trans. American Society of Me-*

- chanical Engineers (ASME)*, Vol.75, No. 4, p. 635-641.
- HITE, J.E., and MIH, W.C. (1994). Velocity of air-core vortices at hydraulic intakes. *Journal of Hydraulic Engineering*, ASCE, Vol.120, No.3, p.284-297.
- JAIN, A.K., RANGA RAJU, K.G., and GARDE, R.J. (1978). Vortex formation at vertical pipe intakes. *Journal of Hydraulic Division*, ASCE, Vol.104, No.10, p. 1429-1448.
- ODGAARD, A.J. (1986). Free surface air core vortex. *Journal of Hydraulic Engineering*, ASCE, Vol.112, No.7, p.610-620.
- YILDIRIM, N., and JAIN, S.C. (1979). Effect of a surface layer on free surface vortex. *Proceedings of the 18th International Association for Hydraulic Research*, Vol.4, p. 411-418, Int. Assoc. for Hydr. Res., Delft, The Netherlands.
- YILDIRIM, N., and KOCABAŞ, F. (1995). Critical submergence for intakes in open channel Flow. *Journal of Hydraulic Engineering*, ASCE, Vol.121, No.12, p.900-905.
- YILDIRIM, N., and KOCABAŞ, F. (1998). Critical submergence for intakes in still-water reservoir. *Journal of Hydraulic Engineering*, ASCE, Vol.124, No.1, p. 103-104.
- YILDIRIM, N., and KOCABAŞ, F. (2000). Flow-boundary effects on critical submergence of an intake pipe. *Journal of Hydraulic Engineering*, ASCE, Vol. 126, No.4, p. 288-297.
- YUAN, S.W. (1967). *Foundation of fluid mechanics*. Prentice-Hall Inc., Englewood Cliffs, N.J.

Appendix I. Geometrical derivations for CSSS II

Geometrical derivations for CSSS II are exactly the same as that of CSSS I which is presented in Appendix III of Yıldırım et al. (2000). The only difference is that the radius of the CSSS II is $r_s = S_c/\sqrt{2}$ (not S_c). Therefore, replace S_c by $r_s = S_c/\sqrt{2}$ in all expressions given in their Appendix III; \overline{JH} , $\overline{K_1Z_1}$, $\overline{K_2Z_2}$, $\overline{K_3Z_3}$, $\overline{K_4Z_4}$ and related expressions for CSSS II are obtained as below.

$$\frac{\overline{JH}}{D_i} = \frac{1}{\sqrt{2}} \frac{S_c}{D_i} - \frac{1}{\sqrt{2}}$$

$$\sqrt{\frac{1}{2} \left(\frac{S_c}{D_i} \right)^2 + \left(\frac{c}{D_i} \right)^2} \sqrt{\frac{1}{2} \left(\frac{S_c}{D_i} \right)^2 - \left(\frac{l}{D_i} \right)^2} + \left(\frac{l}{D_i} \right) \sqrt{\frac{1}{2} \left(\frac{S_c}{D_i} \right)^2 - \left(\frac{c}{D_i} \right)^2}$$
(31)

As it is seen in Fig.3, there will not be the blockage of FHG for the case below.

$$\left(r_s / D_i \right)^2 \leq \left[(c/D_i)^2 + (l/D_i)^2 \right]; \text{ or } \left(S_c / D_i \right)^2 \leq 2 \left[(c/D_i)^2 + (l/D_i)^2 \right]; \text{ FHG} = 0 \text{ and } \overline{JH} = 0.$$

$$\frac{\overline{K_1Z_1}}{D_i} = \frac{1}{\sqrt{2}} \frac{S_c}{D_i} - \frac{1}{\sqrt{2}}$$

$$\sqrt{\frac{1}{2} \left(\frac{S_c}{D_i} \right)^2 + \left(\frac{l}{D_i} \right)^2} \sqrt{\frac{1}{2} \left(\frac{S_c}{D_i} \right)^2 - \left(\frac{b_1}{D_i} \right)^2} + \left(\frac{b_1}{D_i} \right) \sqrt{\frac{1}{2} \left(\frac{S_c}{D_i} \right)^2 - \left(\frac{l}{D_i} \right)^2}$$
(32)

As it is seen in Fig.3, there will not be the blockage of $S_1Z_1B_1$ for the case below.

$$\left(r_s / D_i \right)^2 \leq \left[(b_1/D_i)^2 + (l/D_i)^2 \right]; \text{ or } \left(S_c / D_i \right)^2 \leq 2 \left[(b_1/D_i)^2 + (l/D_i)^2 \right]; \text{ } S_1Z_1B_1 = 0 \text{ and } \overline{K_1Z_1} = 0$$

[for more details see Yıldırım et al. (2000)].

$$\frac{\overline{K_2Z_2}}{D_i} = \frac{1}{\sqrt{2}} \frac{S_c}{D_i} - \frac{1}{\sqrt{2}}$$

$$\sqrt{\frac{1}{2} \left(\frac{S_c}{D_i} \right)^2 + \left(\frac{l}{D_i} \right)^2} \sqrt{\frac{1}{2} \left(\frac{S_c}{D_i} \right)^2 - \left(\frac{b_2}{D_i} \right)^2} + \left(\frac{b_2}{D_i} \right) \sqrt{\frac{1}{2} \left(\frac{S_c}{D_i} \right)^2 - \left(\frac{l}{D_i} \right)^2}$$
(33)

As it is seen in Fig.3, there will not be the blockage of $S_2Z_2B_2$ for the case below.

$$\left(r_s / D_i \right)^2 \leq \left[(b_2/D_i)^2 + (l/D_i)^2 \right]; \text{ or } \left(S_c / D_i \right)^2 \leq 2 \left[(b_2/D_i)^2 + (l/D_i)^2 \right]; \text{ } S_2Z_2B_2 = 0 \text{ and } \overline{K_2Z_2} = 0$$

Similarly, from Fig.3 one can find $\overline{K_3Z_3}$ and $\overline{K_4Z_4}$ as following;

$$\frac{\overline{K_3Z_3}}{D_i} = \frac{1}{\sqrt{2}} \frac{S_c}{D_i} - \frac{1}{\sqrt{2}}$$

$$\sqrt{\frac{1}{2} \left(\frac{S_c}{D_i} \right)^2 + \left(\frac{c}{D_i} \right)^2} \sqrt{\frac{1}{2} \left(\frac{S_c}{D_i} \right)^2 - \left(\frac{b_1}{D_i} \right)^2} + \left(\frac{b_1}{D_i} \right) \sqrt{\frac{1}{2} \left(\frac{S_c}{D_i} \right)^2 - \left(\frac{c}{D_i} \right)^2}$$
(34)

As it is seen in Fig.3, there will not be the blockage of $S_3Z_3B_3$ for the case below.

$$\left(r_s / D_i \right)^2 \leq \left[(c/D_i)^2 + (b_1/D_i)^2 \right]; \text{ or } \left(S_c / D_i \right)^2 \leq 2 \left[(c/D_i)^2 + (b_1/D_i)^2 \right]; \text{ } S_3Z_3B_3 = 0 \text{ and } \overline{K_3Z_3} = 0$$

$$\frac{\overline{K_4 Z_4}}{D_i} = \frac{1}{\sqrt{2}} \frac{S_c}{D_i} - \frac{1}{\sqrt{2}}$$

$$\sqrt{\frac{1}{2} \left(\frac{S_c}{D_i} \right)^2 + \left(\frac{c}{D_i} \right)^2} \sqrt{\frac{1}{2} \left(\frac{S_c}{D_i} \right)^2 - \left(\frac{b_2}{D_i} \right)^2} + \left(\frac{b_2}{D_i} \right) \sqrt{\frac{1}{2} \left(\frac{S_c}{D_i} \right)^2 - \left(\frac{c}{D_i} \right)^2}$$
(35)

As it is seen in Fig.3, there will not be the blockage of $S_4 Z_4 B_4$ for the case below.

$$(r_s / D_i)^2 \leq [(c / D_i)^2 + (b_2 / D_i)^2]; \text{ or } (S_c / D_i)^2 \leq 2[(c / D_i)^2 + (b_2 / D_i)^2]; S_4 Z_4 B_4 = 0 \text{ and } \overline{K_4 Z_4} = 0$$